Organosilane Self-Assembled Multilayer Formation Based on Activation of Methyl-Terminated Surface with Reactive Oxygen Species Generated by Vacuum Ultra-Violet Excitation of Atmospheric Oxygen Molecules

Young-Jong KIM[a,*], Jiwon HAN[a], Hikaru SANO[a], Kyung-Hwang LEE[b],

Kei NODA[c], Takashi ICHII[a], Kuniaki MURASE[a],

Kazumi MATSUSHIGE[c], and Hiroyuki SUGIMURA[a]

[a]Department of Materials Science and Engineering, Kyoto University,

Yoshida-hommachi, Sakyo-ku, Kyoto 606-8501, Japan

[b]Research Institute of Industrial Science and Technology,

Maegok, Buk-gu, Ulsan 683-420, Korea

[c]Department of Electronic Science and Engineering, Kyoto University Katsura,

Nishikyo, Kyoto 615-8510, Japan

*E-mail address : kyj@kyjguide.mbox.media.kyoto-u.ac.jp

Abstract

A xenon excimer lamp which irradiates vacuum ultraviolet (VUV) light at 172 nm in wavelength was applied to the photochemical surface conversion of *n*-octadecyltrimethoxysilane self-assembled monolayer (ODS-SAM) in the presence of atmospheric oxygen and subsequent multilayer fabrication. The terminal functional groups of ODS-SAM, $–CH_3$ groups, were converted into polar functional groups, like –COOH, by the reaction with atomic oxygen species generated photochemically through VUV excitation of atmospheric oxygen molecules. The structure of the resulting organosilane multilayer with different numbers of superimposed monolayers (from 1 to 11), prepared on a smooth and hydrophilic silicon substrate by the layer-by-layer (LbL) approach, was examined in terms of molecular organization as well as the intra- or interlayer binding modes in such novel films. Ellipsometry and grazing angle X-ray reflectivity measurements revealed that multilayer films of up to 11 discrete monolayers were successfully obtained, indicating that the self-assembly is a viable technique for the construction of relatively thick (16 nm and above) multilayer films.

Keywords: self-assembled monolayer (SAM); multilayer; photochemical surface modification; vacuum ultraviolet (VUV); active oxygen species; layer-by-layer approach

1. Introduction

Organized molecular films have attracted growing attention owing to their functionalities in a wide variety of science and engineering fields [1–3]. Such films provide the opportunity for developing new material surface functions leading to improved performance or crucial functions. As a technique for the fabrication of organized molecular films, self-assembly, that is, the spontaneous organization of organic molecules at a solid substrate surface, has been indispensable, as has the Langmuir-Blodgett (LB) method. The self-assembling process is a powerful means for the fabrication on films of a monomolecular thickness, that is, self-assembled monolayer (SAM). However, the process has difficulties in fabricating multilayers compared with the LB method by which multilayers are readily fabricated. Multilayers are expected to yield fruitful functions which cannot be obtained by the monolayers alone. One promising approach to fabricate self-assembled multilayers is the use of coordination chemistry [4]. For example, several types of multilayers have been fabricated through coordination bonds between metal ions with isocyanide or amino groups [5–8]. Mallouk and coworkers developed a promising method in which monolayers of alkyl-bisphosphonic acid and zirconium (Zr) ions were alternately stacked [9]. Besides phosphonic acid, carboxylic acid has been employed in order to fabricate multilayers with Cu(II) or Zr(IV), Ti(IV) ions [10–12]. Although this coordination multilayer chemistry is successful, it lacks versatility since the method needs a bisphosphoric or biscarboxylic molecule as a component of multilayers.

Organosilane SAMs formed on oxide surfaces through the silane coupling chemistry have become a major category of SAM [13–16], and a variety of organosilane precursors are commercially available at present. Thus, multilayer stacking of organosilane SAMs is of special interest. There have been several reports on the fabrication of self-assembled multilayers by the use of an organosilane SAM as the bottom layer of the multilayers [17–26]. In these reported methods, an activation of the bottom SAM surface via chemical or photochemical treatments is frequently applied before stacking an upper layer on it. Thus, there are some requirements for the surface functional groups terminating the bottom SAM; the surface groups must be chemically reactive, or convertible through some chemical treatment processes. If a more general way independent of specific functional groups on a SAM for its activation is available, we can fabricate multilayers more freely. We have reported previously a photochemical surface modification method which could activate even methyl groups on an alkylsilane SAM surface. Organosilane self-assembled bilayers have been fabricated by this method [27–29]. Our photochemical process employs a vacuum ultra-violet (VUV) light at 172 nm in wavelength as a light source. When an organosilane SAM surface is irradiated with VUV light in the presence of atmospheric oxygen molecules, the VUV light excites oxygen molecules, resulting in the generation of ozone molecules as well as oxygen atoms in singlet and triplet states [30]. Since these active oxygen species, particularly singlet oxygen atoms, have strong oxidative reactivity, the species oxidize and etch the monolayer [31]. At the initial stage of this VUV-induced photochemical degradation, surface terminating functional groups of a SAM, e.g., $–CH_3$ or $–CH_2Cl$

groups, are converted to polar functional groups such as –COOH and –CHO. Consequently, the SAM surface becomes hydrophilic to some extent, and this hydrophilically modified SAM surface provides new silane coupling sites for stacking a second organosilane monolayer in order to fabricate a bilayer.

In this paper, we report on a further extension of the VUV-photochemical method to the fabrication of multilayers with more than ten layers. Alkylsilane self-assembled multilayers were successfully fabricated by repeated stacking of alkylsilane layers on the modified SAM surface with hydrophilic conversion of the stacked layer. The structures and properties of the fabricated multilayers are investigated in detail.

2. Experimental

2.1. Samples

We employed an organosilane self-assembled monolayer (SAM) prepared on a silicon (Si) substrate from ODS (*n*-octadecyltrimethoxysilane, $CH_3(CH_2)_{17}Si(OCH_3)_3$, Gelest Inc.) as the first layer for multilayer formation. By using a chemical vapor deposition (CVD) method [32], an ODS-SAM was prepared on Si(100) substrates (phosphorus-doped n-type wafers with a resistivity of 1-11 Ω cm) and Si(111) substrates (phosphorus-doped n-type wafers with a resistivity of 1-10 Ω cm) covered with a 2.3-nm-thick native oxide layer. The Si(111) substrates were used for fourier transform infrared spectroscopy (FTIR) and grazing incidence X-ray reflectivity (GIXR) measurements as described later. All the substrates cut from the wafer were

cleaned ultrasonically with ethanol and ultrapure water for 20 min in this order and then photochemically cleaned by exposing in air to vacuum ultraviolet (VUV) generated from an excimer lamp (Ushio. Inc., UER20-172V; intensity at lamp window 10 mW cm^{-2}) for 20 min at a lamp-sample distance of 5 mm. This photochemical cleaning method is described in detail elsewhere [32]. In a nitrogen-filled glove with a regulated humidity of around 17%, the sample and 60 µL of ODS liquid in a glass cup with a volume of 3 cm^3 were placed in a Teflon container with a capacity of 120 cm^3. The container was then sealed with a screw cap and placed in an electric oven maintained at 150 ˚C for 3 h. The ODS liquid in the vessel vaporized and reacted with –OH groups on the silicon sample surfaces. The molecules were fixed onto the sample surfaces and connected to adjacent ODS molecules through siloxane bonds. ODS-SAM formation was confirmed by the increase in the contact angle from 0 to 104˚ on average, and the thickness estimated by ellipsometry was about 1.4 – 1.5 nm using a model of Air/SiO_2/Si. Detailed properties of the vapor-phase grown ODS-SAMs have already been reported [33,34].

The resulting ODS-SAM on the Si substrate was then treated with another VUV-light process as described later. After the VUV-light treatment, we attempted to stack another ODS-SAM using a silane coupling method, in which the terminal groups of the oxidized ODS-SAM surface, –COOH, –CHO, and/or –CH_2OH groups, acted as new reaction sites. To build a multilayer, the procedure of oxidizing and deposition described above was sequentially repeated. In the final step, the film was capped with an ODS monolayer, creating a chemically inert and nonwettable outer film surface.

2.2. Chemical and physical properties analysis

The static water contact angles of the sample surfaces were measured with a contact angle meter (Kyowa Interface Science, CA-X) in an atmospheric environment; here, we fixed the size of water droplets at about 1.5 mm in diameter. SAM thickness was measured by ellipsometry (Otsuka Electronics, FE-5000). The measured region was 400 – 800 nm in wavelength. The incident angle was set at 70˚, and the model of Air/SiO_2/Si was used for the analysis of raw data. Since the resulting value was the sum of the thickness of the monolayer and the native oxide, the actual monolayer thickness was determined by subtracting the oxide thickness from the total value. Before monolayer coating, the thickness of the native oxide layer of each sample was measured. The chemical bonding states of each sample were examined by X-ray photoelectron spectroscopy (XPS; Kratos Analytical, ESCA-3400) using a Mg Kα X-ray source with 10 mA in emission current and 10 kV in accelerating voltage. The binding energy scales were referenced to 285.0 eV as determined by the locations of the maximum peaks on the C 1s spectra of hydrocarbon (CH_x), associated with adventitious contamination. The LbL self-assembly process was also monitored by quantitative fourier transform infrared spectroscopy (FTIR; Digilab Japan Co., Ltd, Excalibur FTS-3000). We used transmittance mode and a single reflection ATR (attenuated total reflection) mode for measurement of the samples. The ATR IR spectra were obtained with incident angle of 65˚, and hemispherical Ge ATR crystal with diameter of 2.5 cm (internal reflection element, from Harrick Scientific). The transmittance IR spectra

were obtained on 0° incidence. IR Spectra were measured in a dry atmosphere of a sample compartment purged with nitrogen and were referenced to background spectra determined under the same conditions. All spectra were measured at a resolution of 4 cm^{-1} with 1024 scan cycles. The density, thickness, and roughness of the films including oxide-layer on the samples were examined by grazing incidence X-ray reflectivity measurement (GIXR; Rigaku, ATX-G) performed using a high-resolution 18 kW rotating anode X-ray diffractometer. The Cu Kα beam from the rotating anode was monochromatized with flat Ge(220) double crystals. The specular reflectivity curves were recorded with a θ/2θ scan mode. The morphology and surface roughness of the samples were also measured by atomic force microscopy (AFM; SII Nanotechnology, SPA-300HV + SPI-3800N) in tapping mode with a Si probe (Seiko Instruments Inc., SI-DF20, force constant of 15 N m^{-1}).

3. Results and discussion

3.1. Chemical conversion of ODS-SAM

Fig. 1 illustrates the growth mechanism of a solid-immobilized multilayer of oriented long-chain silane molecules, i.e. ODS. Here, "oxidized ODS" means ODS layer treated with VUV-generated active oxygen, and ODS(oxidized ODS)$_n$ denotes the resulting multilayer consisting of n+1 monolayers in total. While the initial cleaning of the Si substrate was done by VUV-irradiation at a lamp-sample distance of 5 mm as described above, VUV-light treatment for the chemical conversion of ODS-SAMs was always

carried out under the larger distance of 30 mm. We employed an excimer lamp as the source of VUV light with wavelength 172 nm, and the chamber was filled with ambient air. The optical absorption coefficient of the VUV light at wavelength 172 nm in ambient air with an oxygen partial pressure of 0.2 atm was reported to be in the range of 10-15 $cm^{-1} atm^{-1}$ [34], indicating that the transmittance of light through a 10 mm-thick air layer would be in the range of 5 -13%, and we observed a value of about 10%. Therefore, the transmittance for 30 mm was estimated to be less than 0.1%, which means that the light intensity at the ODS-SAM surface is less than 0.010 mW cm^{-2}. In other words, at the distance of 30 mm, VUV light was absorbed almost completely by atmospheric oxygen molecules, yielding active oxygen species such as ozone and atomic oxygen, hence no substantial amount of VUV-light reached directly the sample surface. The direct irradiation of ODS-SAMs with VUV photons is not expected in the present system, and only the VUV-light-generated active oxygen can participate in the surface modification of the ODS-SAMs.

In our previous tentative study [29], we have optimized the irradiation time for the chemical conversion [29], using this VUV-light system. Here, it was found that, under the VUV-light treatment, both the water contact angle and the film thickness of the ODS-SAM decreased monotonically with increasing irradiation time. This demonstrated that polar functional groups are evidently and progressively introduced through the treatment with the concomitant etching of the SAM. The introduction of the polar functional groups was also confirmed by XPS measurement [29]. As a result, it was thought that the surface density of polar functional groups, which serve as silane

coupling sites for stacking a second monolayer, is insufficient if the irradiation time is too short. In contrast, if the irradiation time is too long, the second monolayer would be successfully prepared, but the total thickness of the resulting bilayer film will be small. In consequence, the total thickness of the bilayer films grown on VUV-light-treated ODS-SAM substrates was found to increase toward the irradiation time of 400 s and decrease after 400 s until a treatment time of 1200 s. We thus concluded that 400 s is the optimum VUV-light-treatment time. Under this condition, we can introduce maximum polar functional groups on the surface of the first monolayer and, at the same time, minimize the loss of the thickness of the monolayer due to etching.

3.2. Surface analysis of monolayer/multilayers

We prepared eleven different monolayer/multilayers, i.e. ODS(oxidized ODS)$_n$, n = 0-10, through the LbL growth process. Fig. 2 shows the change in water contact angle and thickness of the ODS/(oxidized ODS)$_n$/Si films. The film thickness increased throughout the LbL growth process, and almost proportional relationship was found between the film thickness and the layer number, indicating that a series of multilayers were successfully fabricated on the silicon wafer through the LbL approach. The water contact angle is an indicator of surface wettability, which reflects the surface functional group(s). It is known that the water contact angle for a hydrophobic methyl-terminated surface, e.g. ODS-SAM, is about 105° or more, while that for a surface terminated with a polar functional group is much smaller; for example, oxidized ODS monolayer

obtained by the VUV-light-treatment for 400 s was 36˚ [29]. In the n range of 0 to 10, that is 1 to 11 layers, the water contact angles were around 100˚, suggesting that the layers were throughly terminated with $–CH_3$ groups.

Fig. 3 shows XPS C 1s and Si 2p spectra of initial monolayer (n = 0; 1 layer) and multilayer samples of 4 (n = 3), 7 (n = 6), and 11 layers (n = 10). With increasing layer number, the analyzed amount of carbon at the sample surface increased whereas that of silicon at 99.6 eV, which is mainly due to the Si substrate underneath, decreased, indicating that layers are successfully deposited throughout the LbL self-assembly process, as shown by the water contact angle measurement and the ellipsometric measurement. Here, the difference in C 1s peak intensity between 7 and 11 layers is very small. XPS is a surface sensitive analysis and our system has a detection depth of about 5 nm for organic compounds. As shown in Fig. 2b, the thickness for 11 layers far exceeds 10 nm, resulting in little difference in C 1s intensity between the two samples. For the same reason, the bulk Si peak at 99.6 eV almost disappeared in the case of 11 layers.

The stepwise growth of multilayer films by the sequence of surface oxidizing and layer deposition is also demonstrated by FTIR spectra after each deposition operation of the layer. The FTIR data provide direct evidence for the total amount of film-forming moieties of ODS molecules which are deposited on the surface, and for the orientation and packing density of the ODS paraffnic tails, i.e. hydrocarbon chains, in each deposited layer. Fig. 4 shows FTIR-transmission spectra in the C-H stretching region for the series of the ODS/(oxidized ODS)$_n$/Si (with n = 0, 3, 6, 10) films. The strong

bands observed at 2924 cm^{-1} and 2853 cm^{-1} are assigned to the methylene antisymmetric (ν_aCH_2) and symmetric (ν_sCH_2) stretching modes, respectively. The increasing trends observed in both absorbance intensity of the CH_2 stretch bands arise from variations in the amount of hydrocarbon in the films. From this viewpoint, we can state that layers are deposited in the LbL manner as we predicted. In addition, we can discuss the information that can be obtained from the peak position of these two bands: The peak position of these bands is known to depend on chain-length and the conformation of the paraffinic tails. For example, a shift to higher frequency in the peak positions of the ν_aCH_2 and ν_sCH_2 bands, if any, indicates the reduction of packing density [35]. In the case of Fig. 4 the peak positions of the ν_aCH_2 and ν_sCH_2 bands in all of the spectra are recognized at almost constant wavenumbers of 2924 and 2853 cm^{-1}.

The assembly of mono- and multilayer films, according to the build-up process shown in Fig. 1, was also examined by the FTIR measurement in the attenuated total reflection (ATR) mode, with spectra being taken after the adsorption of each new monolayer, as demonstrated in Fig. 5. By using sufficiently thin Si substrates with thickness 525 μm, in the ATR mode, it became possible to explore the spectral region below 1400 cm^{-1}, which provides important information on the modes of intra- and interlayer bindings. The spectral region below 1400 cm^{-1} is usually inaccessible, because of the strong absorption of the Si substrate itself. The CH_2 stretch bands of the paraffinic chains, peaking at 2926 and 2854 cm^{-1}, which are indicative of the amount of absorbed hydrocarbon material on the surface, were also observed as in the case of FTIR with

transmittance mode. From the spectra given in Fig. 5, the bandwidths and peak positions of the CH_2 stretch bands, at 2926 and 2854 cm^{-1}, did not change against the number of stacked layers, implying that the organization of the hydrocarbon molecular tails is equivalent in all films regardless of total film thickness. A small CH_3 peak at 2955 cm^{-1} was, however, clearly recognized only in the 1 layer spectrum and was hardly seen in the spectra for 4, 7, and 11 layers, since the relative amount of CH_3 groups, which should only exist as the terminal groups of the top most layer, was smaller than in these three samples. The CH_3 peak is, accordingly, hidden in the CH_2 peak shoulder. The 1850 - 750 cm^{-1} spectral region in Fig. 5 provides information on functional groups involved in the intralayer, interlayer, and film-to-surface binding. The presence of both siloxane (Si-O-Si) stretching modes at around 1129 cm^{-1} and a Si-OH stretch band at 880 cm^{-1} indicates the presence of incomplete intra- and interlayer covalent bonding of the silane groups. The broad bands at around 1129 cm^{-1} are characteristic of the Si-O-Si stretching mode of partially condensed oligomeric polysiloxanols. The positions, widths, and intensities of the Si-O-Si bands depend on a number of structural parameters, such as the extent of polymerization, branching, and the nature of the alkyl substituents on the silicon. Most probably, each layer of silane head groups in the present films may be viewed as a two-dimensional network made up of various linear and cyclic polysiloxanol species, which together contribute to the complex features observed in this spectral region. The distribution of siloxane structures in the initial monolayer (1 layer) differs from that in the spectra of the 4, 7, and 11 layer samples, implying differences in the amounts of siloxane bonds originating

from bonds in the interfaces of each layer. The broad band at around 880 cm^{-1} in 1, 4, 7, and 11 layer spectra arises from the Si-OH stretching vibration of unreacted silanols, with contributions from the out-of-plane deformation of the acid OH groups. The feature near 1465 cm^{-1} in all of the spectra is assigned to CH_2 scissoring (δ) vibrations of the alkyl chains. The $\delta(CH_2)$ bending mode is dependent on the lateral packing order of the chains, hence the identical peak positions of $\delta(CH_2)$ in Fig. 5 further confirm the presence of similar two-dimensional packing ordering in these samples, regardless of the structure of the film which would change against the total number of stacked layers.

Excellent depth resolution at the nanometer level is required for surface chemical analysis techniques, where high quality reference material, such as multilayered thin films, is desirable for the optimization of sputter depth profiling. In addition, precise detection of growth processes from the viewpoint of layer thickness, surface and interface roughness with high resolution is an important task. Therefore, grazing incidence X-ray reflectivity (GIXR) is a powerful technique for such objectives. GIXR offers high spatial resolution at the sub-nanometer level for the measurement of roughness and thickness. Its high penetration and non-destructive capabilities are very suitable for probing buried interfaces. Here, we demonstrate the GIXR characterization of the samples, and the thickness determined by GIXR was compared with that found by ellipsometry. The roughness features of different interfaces were also characterized by fitting techniques. X-ray reflectivity profiles on the samples of 1, 4, 7, and 11 layer films are shown in Fig. 6. The dotted and solid curves represent the experimental and fitted data, respectively. Obviously, the 1 layer film has the minimum number of the

oscillations. From 1 layer to 11 layers, an oscillating structure (i.e. kiessig fringe) is found and the number of the oscillations gradually increases, demonstrating clearly that increase of the thickness was achieved by the LbL self-assembly process, as indicated by the ellipsometry measurement. Table 1 shows the optimized values of parameters of film density, thickness, and surface and interface roughness obtained from the sample of 11 layers. It should be noted that the average thickness of each layer is 1.3 nm, which is almost consistent with that obtained from ellipsometric analysis, that is, 1.4 nm per layer. The surface roughness of 0.40 nm on the eleventh layer was slightly smaller than that of the interfacial layers. The higher roughness of the interfacial layers compared to the top layer is probably due to the fact that the interfaces involve traces of chemical etching by to VUV-light-generated active oxygen. For the surface roughness obtained by GIXR, we also employed a supplemental roughness measurement by using atomic force microscopy. The morphology and roughness on the sample surfaces of the 1, 4, 7 and 11 layer films are shown in Fig. 7. The surface roughness of the 1 layer film is about 0.18 nm, which is almost same as that of the substrate without covering ODS-SAM. With increasing number of stacked layers, the surface roughness gradually increases. It reaches be 0.29 nm for 11 layers, indicating the small changes of the surface roughness in each monolayer by layer stacking, while from the layers are successfully deposited throughout the LbL self-assembly process.

4. Conclusions

The *n*-octadecyltrimethoxysilane (ODS) self-assembled multilayer formation based on activation of the methyl-terminated surface with reactive oxygen species generated by vacuum ultra-violet excitation of atmospheric oxygen molecules was investigated by water contact angle, ellipsometry, XPS, FTIR, GIXR, and AFM measurements. We have succeeded in fabricating multilayers with a relatively large thickness (16 nm scale and above) by the simple method in which a sample is treated in gas-phase throughout the process and, thus, no solvent is required to be used. It should be noted that any types of organosilane precursors, even methyl-terminated ones, are compatible to our method. These features of the LbL method here we have demonstrated is thought to be advantageous in practical. Furthermore, since we have employed an optical method for surface activation, the LbL method will be readily extendable to micro-fabrication processes [27,28,31] by activating a selected area with the use of a photomask.

Acknowledgements

This work was supported by KAKENHI (Grants-in-Aid for Scientific Research) and Kyoto University Global COE Program, "International Center for Integrated Research and Advanced Education in Materials Science," from the Japan Society for the Promotion of Science (JSPS) and Kyoto-Advanced Nanotechnology Network, supported by “Nanotechnology Network” of the Ministry of Education, Culture, Sports, Science and Technology (MEXT), Japan.

References

[1] J.D. Swalen, D.L. Allara, J.D. Andrade, E.A. Chandross, S. Garoff, J. Israelachvili, T.J. McCarthy, R. Murray, R.F. Pease, J.F. Rabolt, K.J. Wynne, H. Yu, Langmuir 3 (1987) 932.

[2] A. Ulman, Chem. Rev. 96 (1999) 1533.

[3] F. Schreiber, Prog. Surf. Sci. 65 (2000) 151.

[4] M. Haga, T. Yutaka, Trends in Molecular Electrochemistry, A.J.L. Pombeiro, C. Amatore (Eds.), Marcel Dekker, 2004, p. 311.

[5] M. Maskus, H.D. Abruña, Langmuir 12 (1996) 4455.

[6] M.A. Ansell, E.B. Cogan, C.J. Page, Langmuir 16 (2000) 1172.

[7] M. Altman, A.D. Shukla, T. Zubkov, G. Evmenenko, P. Dutta, M.E. van der Boom, J. Am. Chem. Soc. 128 (2006) 7374.

[8] M. Wanunu, S. Livne, A. Vaskevich, I. Rubinstein, Langmuir 22 (2006) 2130.

[9] H. Lee, L.J. Kepley, H.-G. Hong, T.E. Mallouk, J. Am. Chem. Soc. 110 (1988) 618.

[10] S.D. Evans, A. Ulman, K.E. Goppert-Berarducci, L.J. Gerense, J. Am. Chem. Soc. 113 (1991) 2130.

[11] H. Yonezawa, K.-H. Lee, K. Murase, H. Sugimura, Chem Lett. 35 (2006) 1392.

[12] H. Sugimura, H. Yonezawa, S. Asai, Q.-W. Sun, T. Ichii, K.-H. Lee, K. Murase, K. Noda, K. Mastushige, Colloid Surf. A 321 (2008) 249.

[13] J. Sagiv, J. Am. Chem. Soc. 102 (1980) 92.

[14] K. Ogawa, N. Mino, K. Nakajima, Y. Azuma, T. Ohmura, Langmuir 7 (1991) 1473.

[15] S. Onclin, B.J. Ravoo, D.N. Reinhoudt, Angew. Chem. Int. Ed. 44 (2005) 6282.

[16] H. Sugimura, Nanocrystalline Materials: Their Synthesis -Structure-Property Relationships and Applications, Edited by S.C. Tjong, Elesevier, Oxford, 2006, p. 75.

[17] L. Netzer, R. Iscovici, J. Sagiv, Thin Solid Films 99 (1983) 235.

[18] N. Tillman, A. Ulman, J.F. Elman, Langmuir 5 (1989) 1020.

[19] K. Ogawa, N. Mino, H. Tamura, M. Hatada, Langmuir 6 (1990) 851.

[20] W. Lin, W. Lin, G.K. Wong, T.J. Marks, J. Am. Chem. Soc. 118 (1996) 8034.

[21] T. Takahagi, Y. Nagasawa, A. Ishitani, Jpn. J. Appl. Phys. 35 (1996) 3542.

[22] S. Heid, F. Effenberger, Langmuir 12 (1996) 2118.

[23] S. Katom, C. Pac, Langmuir 14 (1998) 2372.

[24] J. Naciri, J.Y. Fang, M. Moore, D. Shenoy, C.S. Dulcey, R. Shashidhar, Chem. Mater. 12 (2000) 3288.

[25] M.-T. Lee, G.S. Ferguson, Langmuir 17 (2001) 762.

[26] T. Lummerstorfer, H. Hoffmann, J. Phys. Chem. B 108 (2004) 3963.

[27] L. Hong, H. Sugimura, T. Furukawa, O. Takai, Langmuir 19 (2003) 1966.

[28] H. Sugimura, L. Hong, K.-H. Lee, Jpn. J. Appl. Phys. 44 (2005) 5185.

[29] Y.-J. Kim, K.-H. Lee, H. Sano, J. Han, T. Ichii, K. Murase, H. Sugimura, Jpn. J. Appl. Phys. 47 (2008) 307.

[30] R.P. Roland, M. Bolle, R.W. Anderson, Chem. Mater. 13 (2001) 2493.

[31] H. Sugimura, K. Ushiyama, A. Hozumi, O. Takai, Langmuir 16 (2000) 885.

[32] H. Sugimura, A. Hozumi, T. Kameyama, O. Takai, Surf. Interf. Anal. 34 (2002) 550.

[33] H. Sugimura, N. Nakagiri, J. Photoplym. Sci. Technol. 10 (1997) 661.

[34] K. Watanabe, E.C.Y. Inn, M. Zelikoff, J. Chem. Phys. 21 (1953) 1026.

[35] C. Naselli, J.F. Rabolt, J.D. Swalen, J. Chem. Phys. 82 (1985) 2136.

Figure Legends

Fig. 1. Conception illustration of the layer-by-layer chemical self-assembly of ODS/(oxidized ODS)$_n$/Si films, where oxidized ODS means ODS-SAM treated with VUV-generated active oxygen in order to convert terminal methyl groups into active groups such as a carboxyl group. Built-up multilayer structures of this kind are composed mainly of oxidized ODS, rather than ODS. Deposition of a final layer of saturated ODS, instead of oxidized ODS, will stabilize the final multilayer structure ((n+1) layers, with a top ODS monolayer, shown on the upper left of figure.).

Fig. 2. Change in (a) water contact angle and (b) thickness of ODS multilayer against number of layers. Measurements were taken with three different samples.

Fig. 3. XPS (a) C 1s and (b) Si 2p spectra of ODS monolayer/multilayer samples with four different numbers of stacked layers.

Fig. 4. FTIR-transmission spectra for ODS monolayer/multilayer samples with four different numbers of stacked layers in the region of 2750 - 3050 cm^{-1}. The spectra were referenced to a common background, and obtained with resolution of 4 cm^{-1} and 1024 scan cycles.

Fig. 5. FTIR-ATR spectra for ODS monolayer/multilayer samples with four different numbers of stacked layers. All the spectra were collected using the same ATR crystal and were referenced to a common background. The resolution was 4 cm^{-1} and the number of scan cycles was 1024.

Fig. 6. A set of measured X-ray reflectivity profiles (dotted curves) and the fitted curves (solid line) for ODS monolayer/multilayer samples with four different numbers of stacked layers.

Fig. 7. AFM topographic images with RMS roughness of ODS monolayer/multilayer samples with four different numbers of stacked layers.

Table Title

Table 1. Structural parameters for the 11 layers film determined by the fitting of GIXR profile

Table 1. Structural parameters for the 11 layers film determined by the fitting of GIXR profile

Layer	Density (g/cm^3)	Thickness (nm)	RMS roughness (nm)
11th layer	0.64	1.2	0.40
10th layer	0.78	1.2	0.42
9th layer	0.82	1.3	0.72
8th layer	0.84	1.3	0.65
7th layer	0.89	1.4	0.77
6th layer	0.91	1.2	0.74
5th layer	0.94	1.2	0.70
4th layer	1.03	1.3	0.73
3rd layer	1.15	1.3	0.70
2nd layer	1.24	1.3	0.69
1st layer	1.23	1.2	0.60
SiO_2	1.08	0.8	0.83
Si	2.25	–	1.18

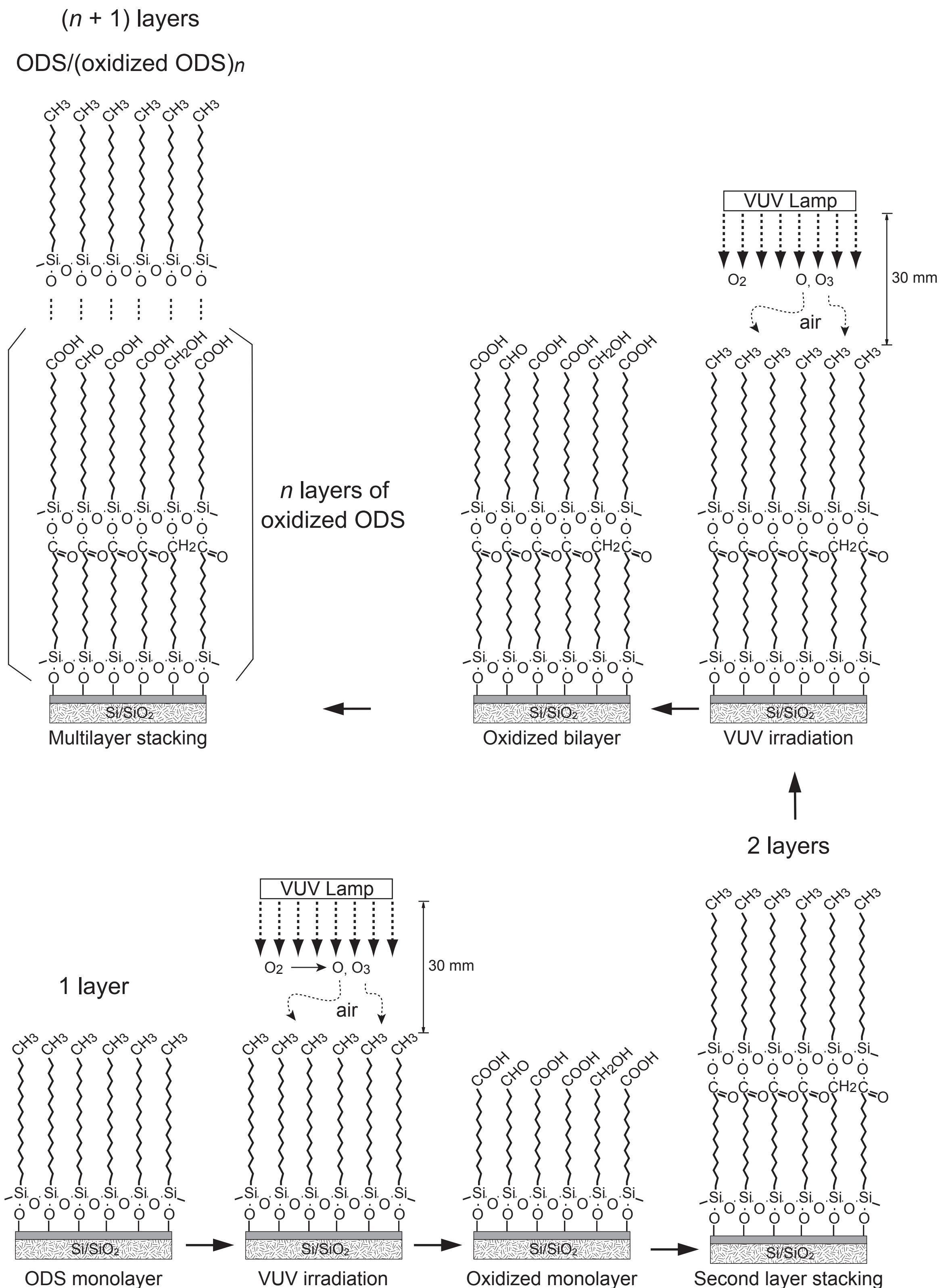

Fig. 1. Conception illustration of the layer-by-layer chemical self-assembly of ODS/(oxidized ODS)n/Si films, where oxidized ODS means ODS-SAM treated with VUV-generated active oxygen in order to convert terminal methyl groups into active groups such as a carboxyl group. Built-up multilayer structures of this kind are composed mainly of oxidized ODS, rather than ODS. Deposition of a final layer of saturated ODS, instead of oxidized ODS, will stabilize the final multilayer structure ((n+1) layers, with a top ODS monolayer, shown on the upper left of figure.).

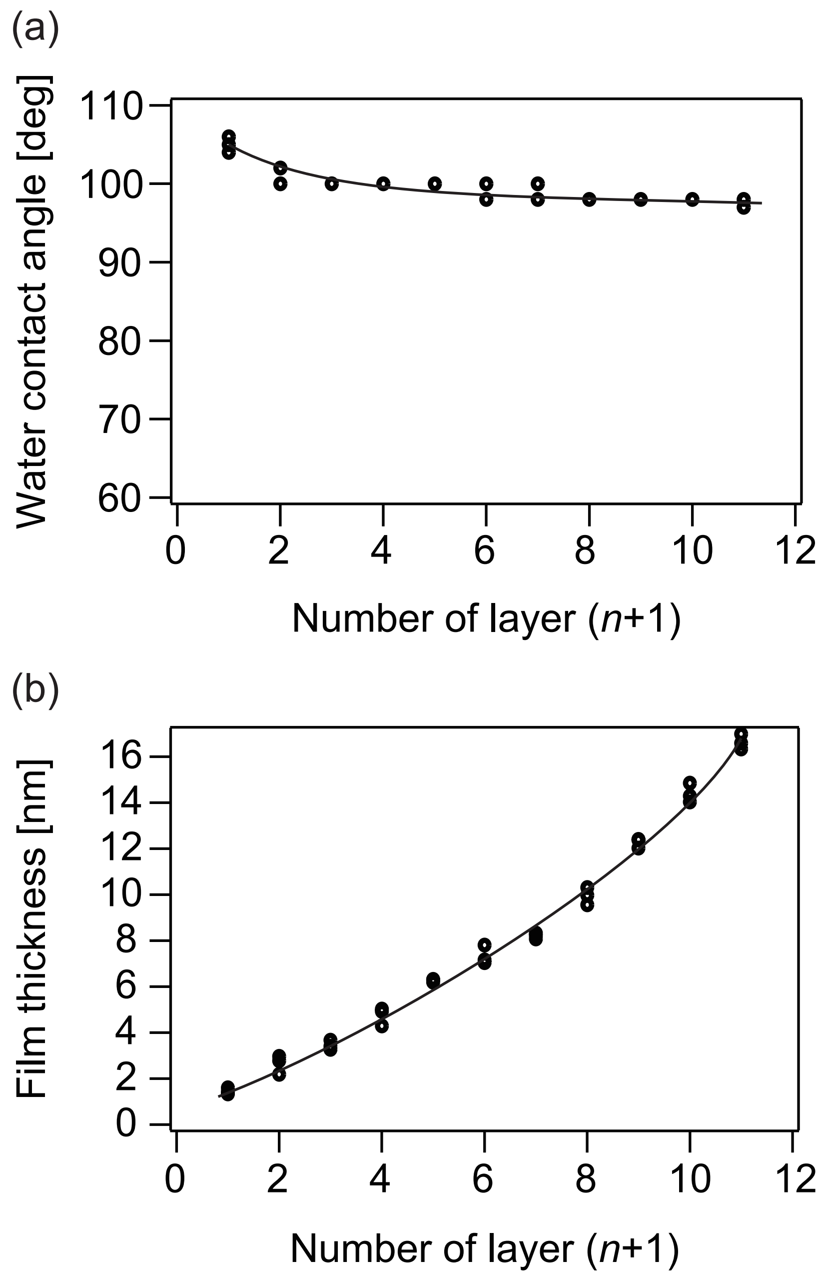

Fig. 2. Change in (a) water contact angle and (b) thickness of ODS multilayer against number of layers. Measurements were taken with three different samples.

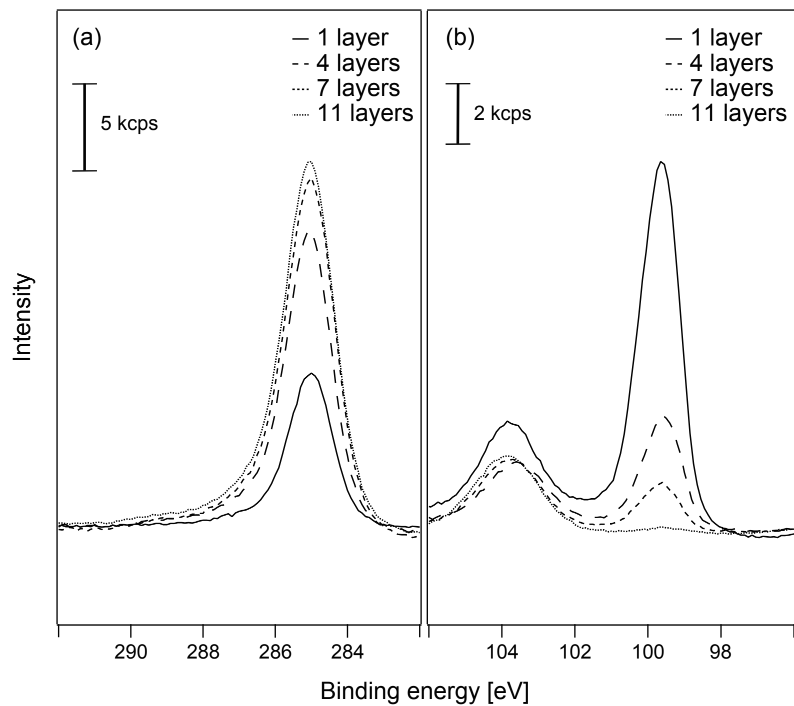

Fig. 3. XPS (a) C 1s and (b) Si 2p spectra of ODS monolayer/multilayer samples with four different numbers of stacked layers.

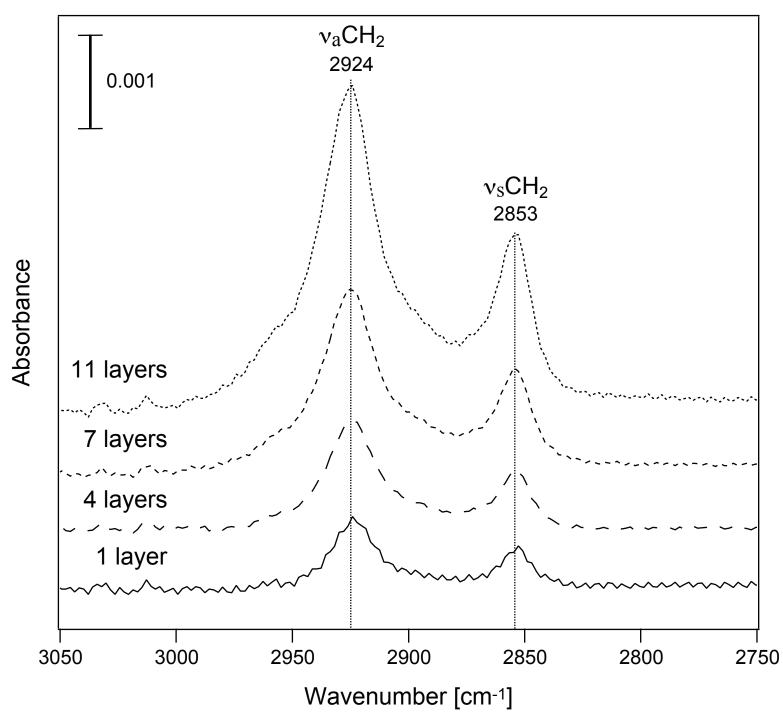

Fig. 4. FTIR-transmission spectra for ODS monolayer/multilayer samples with four different numbers of stacked layers in the region of 2750 - 3050 cm-1. The spectra were referenced to a common background, and obtained with resolution of 4 cm-1 and 1024 scan cycles.

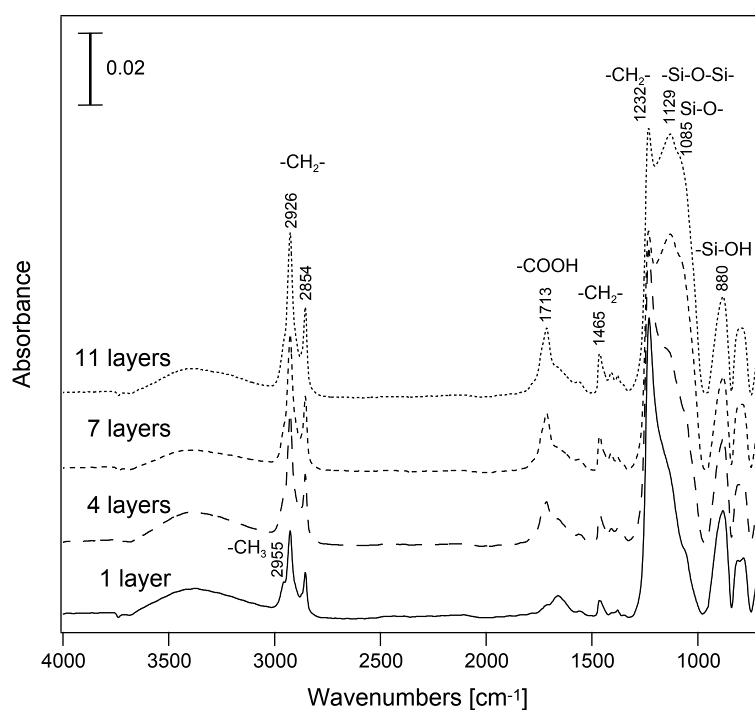

Fig. 5. FTIR-ATR spectra for ODS monolayer/multilayer samples with four different numbers of stacked layers. All the spectra were collected using the same ATR crystal and were referenced to a common background. The resolution was 4 cm-1 and the number of scan cycles was 1024.

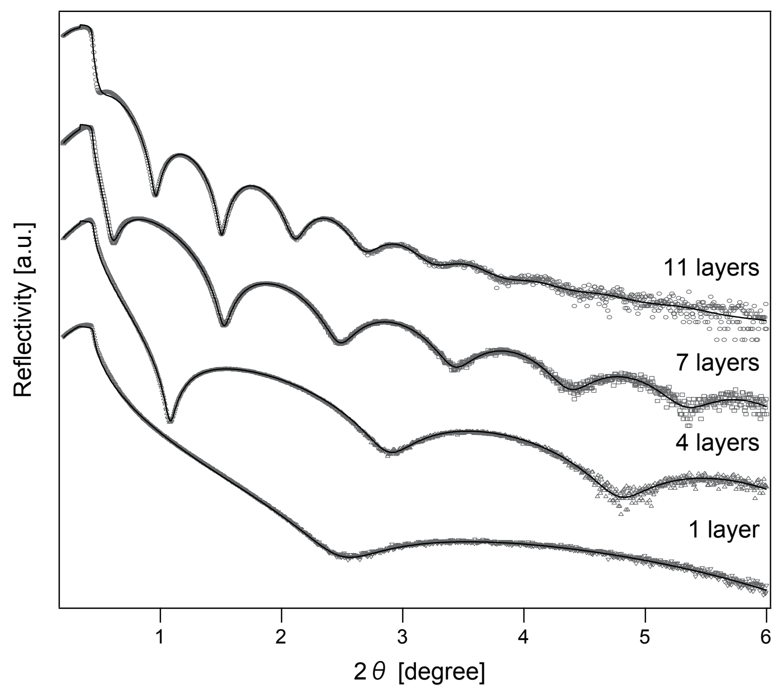

Fig. 6. A set of measured X-ray reflectivity profiles (dotted curves) and the fitted curves (solid line) for ODS monolayer/multilayer samples with four different numbers of stacked layers.

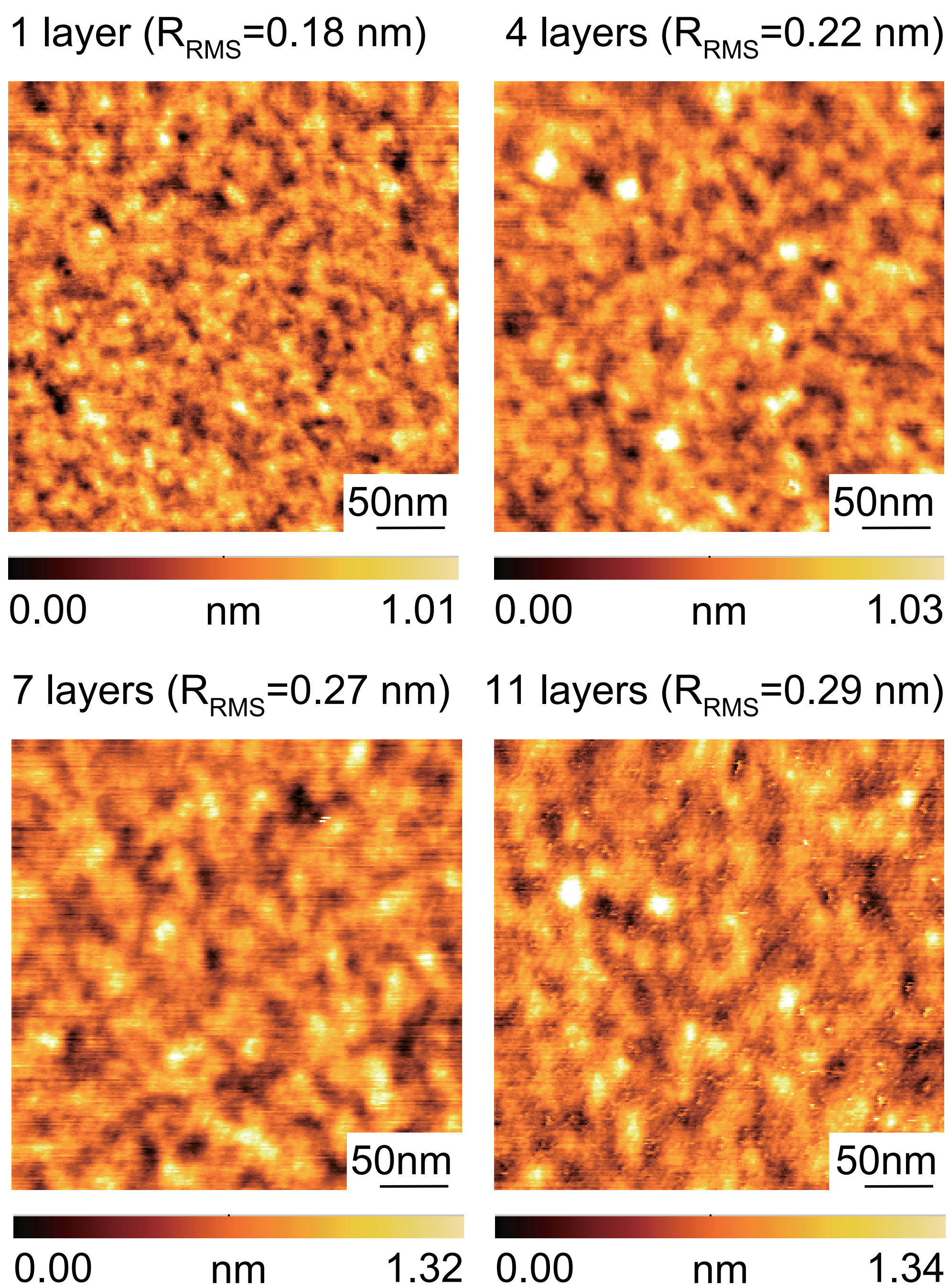

Fig. 7. AFM topographic images with RMS roughness of ODS monolayer/multilayer samples with four different numbers of stacked layers.